# Expedited Metaheuristic-Based Antenna Optimization Using EM Model Resolution Management

Anna Pietrenko-Dabrowska[1][0000-0003-2319-6782], Slawomir Koziel[1,2][0000-0002-9063-2647], and Leifur Leifsson[3][0000-0001-5134-870X]

[1] Faculty of Electronics Telecommunications and Informatics, Gdansk University of Technology, Narutowicza 11/12, 80-233 Gdansk, Poland
`anna.dabrowska@pg.edu.pl`
[2] Engineering Optimization & Modeling Center, Department of Engineering, Reykjavík University, Menntavegur 1, 102 Reykjavík, Iceland
`koziel@ru.is`
[3] School of Aeronautics and Astronautics, Purdue University, West Lafayette, IN 47907, USA
`leifur@purdue.edu`

**Abstract.** Design of modern antenna systems heavily relies on numerical optimization methods. Their primary purpose is performance improvement by tuning of geometry and material parameters of the antenna under study. For reliability, the process has to be conducted using full-wave electromagnetic (EM) simulation models, which are associated with sizable computational expenditures. The problem is aggravated in the case of global optimization, typically carried out using nature-inspired algorithms. To reduce the CPU cost, population-based routines are often combined with surrogate modeling techniques, frequently in the form of machine learning procedures. While offering certain advantages, their efficiency is worsened by the curse of dimensionality and antenna response nonlinearity. In this article, we investigate computational advantages of combining population-based optimization with variable-resolution EM models. Consequently, a model management scheme is developed, which adjusts the discretization level of the antenna under optimization within the continuous spectrum of acceptable fidelities. Starting from the lowest practically useful fidelity, the resolution converges to the highest assumed level when the search process is close to conclusion. Several adjustment profiles are considered to investigate the speedup-reliability trade-offs. Numerical results have been obtained for two microstrip antennas and particle swarm optimizer as a widely-used nature-inspired algorithm. Consistent acceleration of up to eighty percent has been obtained in comparison to the single-resolution version with minor deterioration of the design quality. Another attractive feature of our methodology is versatility and easy implementation and handling.

**Keywords:** Antenna design, global optimization, variable resolution models, EM-driven design, nature-inspired optimization.

# 1   Introduction

Contemporary antenna systems are developed to satisfy stringent performance requirements imposed by existing and emerging applications (internet of things (IoT) [1], body area networks [2], 5G technology [3], implantable devices [4], etc.), enable a range of functionalities (multi-band [5] and MIMO operation [6], reconfigurability [7], beam scanning [8]), and, in many cases, feature compact physical dimensions [9]. Fulfilling such performance demands leads to topologically intricate structures, whose parameters necessitate meticulous tuning. At the same time, they can be reliably evaluated solely using full-wave electromagnetic (EM) analysis. As a matter of fact, EM simulation tools are indispensable at all design stages, starting from geometry evolution, through parametric studies, to final tuning of antenna parameters.

Given the complexity of modern antennas but also the need for handling multiple objectives and constraints, performance-oriented parameter adjustment has to be carried out using rigorous numerical optimization methods [10]. The most problematic issue thereof is high computational cost, which may be troublesome even for local tuning. Global optimization entails incomparably higher expenses, yet it is recommended in a growing number of situations, e.g., design of frequency-selective surfaces [11], array pattern synthesis [12], EM-driven miniaturization [13], re-design of antennas over broad ranges of operating frequencies.

Nowadays, global optimization is primarily conducted using nature-inspired methods [14], [15]. Some of the popular techniques include evolutionary algorithms [16], particle swarm optimizers (PSO) [17], differential evolution (DE) [18], or firefly algorithm [19]. New methods are reported on almost daily basis (e.g., [20]-[22]), yet the differences between them are often cosmetic. The global search capability is arguably a result of exchanging information between candidate solutions processed by the algorithm [23], using exploratory/exploitative operators, as well as mimicking social or biological phenomena [24]. Popularity of nature-inspired methods stems from their simplicity, both in terms of implementation and handling. The downside is remarkably poor computational efficiency. Typical running costs measured in thousands of objective function evaluations are prohibitive from the perspective of EM-driven design. A possible workaround is the incorporation of surrogate modeling [25]-[27]. Shifting the computational burden into a fast metamodel enables acceleration. In practice, iterative procedures, often referred to as machine learning [28], are utilized, where the surrogate serves as predictor which undergoes refinement using the accumulated EM simulation data. The strategies for generating the infill points may be based on parameter space exploration (identifying the most promising regions), exploitation (pursuing the optimum) or combination of both [29]. In the context of global optimization, the employment of metamodels is impeded by the curse of dimensionality, broad ranges of geometry parameters and frequency, as well as antenna response nonlinearity. These can be alleviated by domain confinement [30], [31], variable-fidelity approaches [32], or feature-based methodologies [33], [34].

The mitigation methods mentioned above address some of the problems pertinent to global EM-based antenna design but are not free for the issues on their own. These include, among others, limited versatility and implementation complexity. From this perspective, the employment of variable-resolution models seems to be the simplest yet offering sizable computational benefits. In most cases, it utilizes two levels of fidelity

(equivalent networks vs. EM analysis [35]) or resolution (coarse- and fine-discretization EM simulations [36]). Using a continuous range of model resolutions might be a more flexible option. In the realm of nature-inspired procedures, this idea has been pursued in [37]; however, it was demonstrated mainly using analytical functions.

This article investigates potential merits of incorporating variable-resolution EM analysis into nature-inspired optimization of antenna systems. A model management scheme is developed, which establishes the model fidelity from a continuous spectrum of resolutions. The latter is controlled by a discretization density of the computational model of the antenna under design. The search process starts from the minimum usable resolution and gradually increases it as the algorithm reaches convergence. The speedup-reliability trade-offs can be worked out by adjusting the model selection profile. Numerical experiments have been conducted using two microstrip antennas and a particle swarm optimizer (PSO) as a representative nature-inspired optimization routine. The results demonstrate that the search process can be considerably expedited with cost savings of up to eighty percent as compared to the single-fidelity PSO version. At the same time, design quality degradation is practically negligible. The proposed approach is straightforward to implement and handle, and can be incorporated into any population-based metaheuristic.

## 2  Antenna Optimization. Variable-Resolution Models

In this section, formulation of the antenna optimization problem and introduction of variable-resolution computational models are recalled. The latter are illustrated using a microstrip antenna example.

### 2.1  EM-driven Design. Problem Formulation

In this work, we use the following formulation of the simulation-based antenna optimization task. Given the parameter vector $x$, the aim is to minimize a scalar objective function $U$ quantifying the design quality. The optimum parameter vector $x^*$ is found as

$$x^* = \arg\min_x U(x) \tag{1}$$

Representative examples of optimization scenarios and the associated objective function can be found in Fig. 1. Therein, $f$ stands for the frequency, whereas $|S_{11}(x,f)|$, $G(x,f)$, and $AR(x,f)$ are the reflection coefficient, gain, and axial ratio at design $x$ and frequency $f$; $A(x)$ is the antenna size (e.g., the footprint area). Note that in all cases, the primary objective is directly optimized, whereas secondary objectives are cast into constraints handled using the penalty function approach.

### 2.2  Variable-Resolution EM Models

In the design of antennas and microwave components, variable-resolution EM simulations have been already employed for expediting simulation-driven design optimization procedures [35], [39]. Yet, in majority of frameworks, only two levels of resolution are utilized, i.e., coarse (low-fidelity) and fine (high-fidelity). The performance of any variable-fidelity procedure strongly depends on the evaluation cost and accuracy of the low-fidelity model, whose appropriate selection is a challenging task of fundamental importance [40].

| Design scenario: verbal description | Objective function $U$ |
|---|---|
| Design for best in-band matching within the frequency range $F$ | $U(\boldsymbol{x}) = S(\boldsymbol{x}) = \max\{f \in F : |S_{11}(\boldsymbol{x},f)|\}$ |
| Design for maximum average in-band gain (in frequency range $F$); Ensuring that in-band matching does not exceed $-10$ dB in $F$ | $U(\boldsymbol{x}) = \dfrac{1}{F}\displaystyle\int_F G(\boldsymbol{x},f)df + \beta_1 c_1(\boldsymbol{x})^2$ where $c_1(\boldsymbol{x}) = \left[\dfrac{\max(S(\boldsymbol{x})+10,0)}{10}\right]^2$ |
| Design for size reduction of a circularly polarized antenna; Ensuring that in-band matching (in frequency range $F$) does not exceed $-10$ dB, and axial ratio does not exceed 3 dB, both over the frequency range $F$ | $U_P(\boldsymbol{x}) = \max\{f \in F : A(\boldsymbol{x},f)\} + \beta_1 c_1(\boldsymbol{x})^2 + \beta_2 c_2(\boldsymbol{x})^2$ where $c_1(\boldsymbol{x}) = \left[\dfrac{\max(S(\boldsymbol{x})+10,0)}{10}\right]^2$ and $c_2(\boldsymbol{x}) = \left[\dfrac{\max(\max\{f \in F : AR(\boldsymbol{x},f)\}-3,0)}{3}\right]^2$ |

Fig. 1. Representative antenna design optimization scenarios.
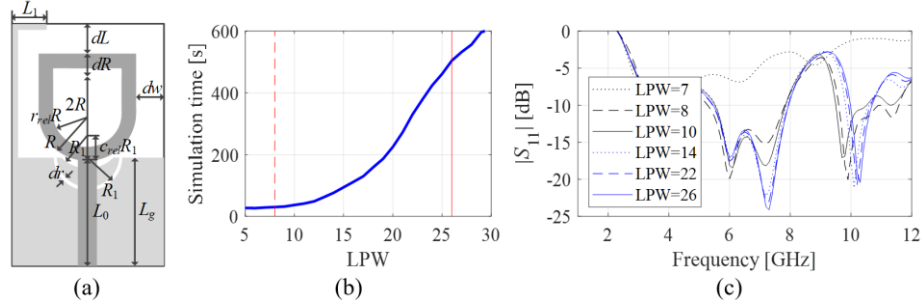


Fig. 2. Multi-resolution EM models: (a) exemplary broadband monopole antenna, (b) average simulation time versus LPW (the vertical lines indicate the values of LPW for the high-fidelity model (—) and the lowest practically useful low-fidelity model (- - -)); (c) reflection responses corresponding to various discretization densities.

Here, the low-fidelity EM models are realized using coarse-discretization EM analysis, which a usual approach in the case of antenna structures. Other possibilities, e.g., equivalent networks or analytical models, are not readily obtainable and difficult to parameterize. In our approach, a major mechanism employed to accelerate the simulation process is a reduction of the model discretization level. Our numerical experiments are carried out using CST Microwave Studio [41], one of the most popular commercial EM solvers. Therein, the discretization density is controlled with the use of a single parameter, LPW (lines per wavelength).

Figure 2 presents an exemplary antenna: its geometry and reflection response $|S_{11}|$ evaluated for various values of the LPW parameter. Both evaluation accuracy and the simulation cost increase with an increase of the LPW value. The acceptable range of model resolutions should be cautiously selected, because below a certain LPW value,

the model is no longer usable due to largely inaccurate rendition of antenna characteristics as shown in Fig. 2. In practice, a visual inspection of family of antenna responses suffices to assess the admissible range of LPW: from $L_{min}$, being the lowest value suitable for carrying out antenna optimization, up to $L_{max}$, i.e., the highest value representing the model of the maximum fidelity. The former is normally estimated as the value for which the respective model accounts for all meaningful features of the antenna response, such as the resonances. Whereas the latter corresponds to the accuracy level deemed adequate by the designer. It is most often estimated as the LPW value increasing of which does not bring in any further changes to antenna responses.

## 3 Population-Based Optimization with Variable-Fidelity EM Models

The aim of this section is to outline the metaheuristic-based antenna optimization technique considered in this work. Section 3.1 delineates a generic structure of nature-inspired optimization procedures, whereas its integration with variable-resolution model management is provided in Section 3.2. Demonstration experiments are delineated in Section 4.

### 3.1 Nature-Inspired Algorithms. Generic Structure

Let us first define the main entities, which are conventionally utilized in virtually any given nature-inspired algorithm. In the $k$th iteration, we have the population $\boldsymbol{P}^{(k)} = [P_1^{(k)} \ldots P_N^{(k)}]$ of size $N$, which, depending on algorithm type, may also be referred to as a swarm or pack. The assumed number of iterations $k_{max}$ defines the computational budget, which, in turn, decides upon algorithm termination. The aim is to minimize the cost function $E(P)$, which quantifies the solution quality. Here, we will use a shortened symbol $E_{k,j}$ instead of a full notation $E(P_j^{(k)})$. In particle swarm optimization algorithm [17], utilized in this work as a base search engine, the best particle found so far is passed over throughout the subsequent iterations (this feature is referred to as elitism).

The particular ways of creating a new population $\boldsymbol{P}^{(k+1)}$ from the previous one vary between different nature-inspired algorithms. For example, in PSO [17] (but also in DE [18], and firefly algorithm [19]), the replacement of the individuals is, in general, not performed. Instead, the individuals are repositioned in the search space according to the assumed rules, usually, by random modifications biased in the direction of the best local and global solutions identified in the previous iterations. In PSO, a velocity vector governing the transfer to a new location is assigned to each particle. The said vector is modified with the use of a linear combination of three factors: (i) a random factor, (ii) a vector in the direction of the best location of a given particle, and (iii) a vector pointing into the direction of the global optimum.

### 3.2 Variable-Resolution Model Management

We aim at accelerating metaheuristic-based optimization procedure delineated in Section 3.1 by exploiting variable-resolution EM models of Section 2.2. In our algorithm, the model resolution $L$ is to be continuously modified (from the minimum value $L_{min}$ to the highest one $L_{max}$) based on the iteration count $k \leq k_{max}$, where $k_{max}$ is the maximum number of iterations. The following adjustment scheme is employed [38]

```
1.   Set the iteration index k = 0;
2.   Set the model resolution L(k) = Lmin;
3.   Initialize population P(k);
4.   Evaluate population P(k) at the resolution level L(k) to find
         Ek,j, j = 1, …, N;
5.   Find the best individual [Pbest, Ebest] in P(k), where Ebest = min{j = 1, …, N :
     Ek,j}, and Pbest is the individual associated with Ebest;
6.   while k < kmax do
7.       Set k = k + 1;
8.       Generate a new population P(k) from P(k–1) using the algorithm-
             specific rules;
9.       Update model resolution L(k) according to (2);
10.      Evaluate population P(k) at the resolution level L(k) to find
             Ek,j, j = 1, …, N;
11.      Evaluate Pbest at the resolution level L(k) to find updated Ebest;
12.      Find the best individual [Pbest.tmp, Ebest.tmp] in P(k);
13.      if Ebest.tmp < Ebest then
14.          Update global best: Pbest = Pbest.tmp and Ebest = Ebest.tmp;
15.  return Pbest and Ebest.
```

Fig. 3. Accelerated nature-inspired algorithm incorporating multi-resolution EM models: pseudocode. The steps specific to the adopted acceleration mechanism: Step 2 (initialization of the model resolution level), Step 9 (adjustment of the current model resolution level), and Step 11 (re-evaluation of the best individual identified so far using the new resolution level). The remaining steps are common for both the basic and accelerated version of the algorithm.

$$L(k) = L_{\min} + (L_{\max} - L_{\min})\left[\frac{k}{k_{\max}}\right]^{p} \tag{2}$$

where $p$ denotes power parameter. The resolution adjustment scheme (2) is sufficiently flexible: (i) for $p > 1$, $L \approx L_{\min}$ throughout majority of optimization course, when close to convergence $L$ quickly increases towards $L_{\max}$; (ii) for $p < 1$, $L_{\min}$ is used only at the beginning of the optimization process, with $L \approx L_{\max}$ utilized throughout the rest of the optimization course.

A pseudocode of an expedited population-based algorithm employing variable-resolution EM models is shown in Fig. 3. At the onset of the optimization process, we set $L = L_{\min}$ (Step 2). Next, the individuals are evaluated at the current resolution level $L(k)$ adjusted according to (2) (Step 9). At the end of the current iteration, the best solution $P_{best}$ is re-evaluated using an updated resolution level, and it is subsequently compared (Step 13) to the best solution from the current population (to ensure that the comparison is carried out at the same resolution level). This is because the individual being the best at previous fidelity level is not necessarily the best at new resolution.

Clearly, it is to be anticipated that the higher the $p$, the higher are potential savings. As a matter of fact, these saving may be assessed a priori. The computational expenditures $T_I$ of the basic single-fidelity algorithm using the fine EM model of resolution $L_{max}$ may be expressed as

$$T_I = N \cdot k_{max} \cdot T(L_{max}) \tag{3}$$

where $T(L_{max})$ refers to the evaluation time of the antenna structure under design at the highest resolution level $L_{max}$ (for any given model fidelity $L$, we denote the corresponding evaluation time as $T(L)$). Whereas the cost of the proposed multi-fidelity optimization procedure equals to

$$T_{II} = N \cdot T(L_{min}) + (N+1)T(L(1)) + (N+2)T(L(2)) + ... + (N+1)T(L(k_{max})) \tag{4}$$

which may be approximated as

$$T_{II} \approx (N+1) \cdot \sum_{k=0}^{k_{max}} T(L(k)) \tag{5}$$

In (5), the multiplier $N+1$ stems from the necessity of re-evaluating the best individual using current $L$ in Step 11.

Let us analyse the algorithm running times predicted using (5) for the antenna of Fig. 2 (see Table 1). The control parameters of the core PSO algorithm are: the population size $N = 10$, with the maximum iteration number $k_{max} = 100$. Observe that both $N$ and $k_{max}$ are kept low (for a typical population-based algorithm). The reason is the necessity to curb the optimization cost as the responses of the antenna structures are evaluated using expensive full-wave EM simulations. Despite the fact that the antenna shown in Fig. 2 is relatively simple, the computational expenses provided in Table 1 are still high (over five days). Such cost level is, however, unavoidable in simulation-driven antenna design. Potential savings due to the proposed accelerated algorithm with respect to basic procedure depend on the power factor $p$. Even for the lowest value of $p = 1$, the anticipated savings reach 50 percent. Whereas for $p = 3$ savings of over 70 percent may be obtained. Decreasing the computational cost to such degree is highly desirable. Yet, the reliability of the proposed multi-fidelity procedure remains to be verified. It is especially of interest, whether and to what extent the computational speedup might be detrimental to the design quality. This is going to be verified in Section 4.

**Table 1.** Estimated cost of a generic metaheuristic-based algorithm for antennas of Fig. 2

| EM model setup | | Computational cost of the optimization process ($N = 10$, $k_{max} = 100$) | |
| --- | --- | --- | --- |
| | | Execution time | Savings w.r.t. single-fidelity-based algorithm |
| High-fidelity ($L = L_{max}$) | | 132.1 h | - |
| Variable resolution | $p = 0.5$ | 82.2 h | 37.7 % |
| | $p = 1.0$ | 57.0 h | 56.8 % |
| | $p = 2.0$ | 37.7 h | 71.5 % |
| | $p = 3.0$ | 29.6 h | 77.6 % |
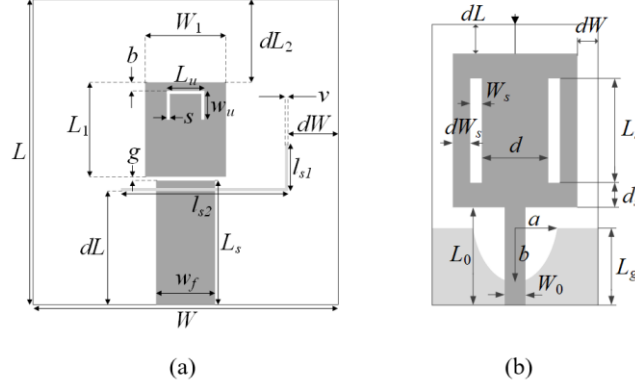
Fig. 4. Antennas used for verification of the introduced porcedure: (a) Antenna I [42],and (b) Antenna II [43] (ground-plane metallization is marked using light grey color).

**Table 2.** Verification antenna structures

| | Case study | |
| --- | --- | --- |
| | Antenna I | Antenna II |
| Substrate | $\varepsilon_r = 3.2$<br>$h = 3.1$ mm | $\varepsilon_r = 4.3$<br>$h = 1.55$ mm |
| Design parameters | $\boldsymbol{x} = [L_1\ L_s\ L_u\ W\ W_1\ dL\ dW\ g\ l_{s1}\ l_{s2}\ w_u]^T$ | $\boldsymbol{x} = [L_g\ L_0\ L_s\ W_s\ d\ dL\ d_s\ dW_s\ dW\ a\ b]^T$ |
| Other parameters | $b = 1, w_f = 7.4,$<br>$s = 0.5, w = 0.5,$<br>$dL_2 = L_1, L = L_s + g + L_1 + dL_2$ | $W_0 = 3.0$ |
| Operating bands | 80 MHz bandwidth centered at frequencies 3.5 GHz, 5.8 GHz, and 7.5 GHz | UWB frequency band from 3.1 GHz to 10.6 GHz |
| Parameter space | $\boldsymbol{l} = [10\ 17\ 5\ 45\ 8\ 15\ 9\ 0.2\ 4\ 20\ 2]^T$<br>$\boldsymbol{u} = [16\ 25\ 8\ 55\ 12\ 20\ 12\ 0.4\ 6\ 24\ 3]^T$ | $\boldsymbol{l} = [5\ 5\ 5\ 0.2\ 0.2\ 5\ 0.3\ 0.5\ 1.0\ 0.1\ 0.2]^T$<br>$\boldsymbol{u} = [15\ 15\ 15\ 1.2\ 8\ 15\ 1.5\ 2.5\ 5\ 0.5\ 0.5]^T$ |
| | Low-fidelity model | |
| $L_{min}$ | 8 | 6 |
| Simulation time [s] | 32 | 33 |
| | High-fidelity model | |
| $L_{max}$ | 25 | 25 |
| Simulation time [s] | 114 | 378 |
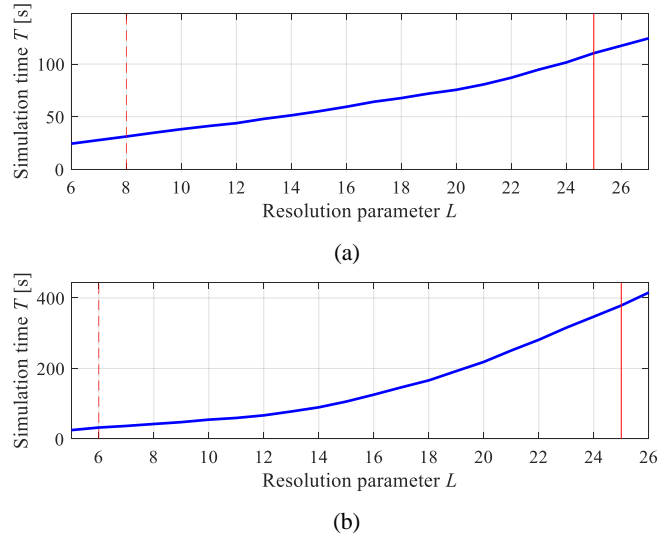
Fig. 5. Relationship of simulation time on EM model fidelity for antennas of Fig. 4: (a) Antenna I, and (b) Antenna II. The resolutions $L_{min}$ (the minimum usable resolution) and $L_{max}$ (the maximum resolution of high-fidelity model) are marked using (- - -) and (—) values, respectively.

## 4 Demonstration Experiments

The introduced multi-resolution metaheuristic-based antenna optimization algorithm delineated in Section 3 is validated using a triple-band antenna (Antenna I), as well as a wideband monopole antenna (Antenna II). The core optimization procedure is the particle swarm optimizer (PSO) [41], which has been selected as a widely utilized population-based technique.

### 4.1 Test Cases

The test antenna structures utilized for numerical validation of our approach are shown in Fig. 4, whereas the relevant details on their parameters, design space (delimited by the vectors $l$ and $b$, i.e., the lower and upper bounds for antenna dimensions, respectively) and objectives, as well as the setup of variable-resolution EM models are provided in Table 2. Antenna I, presented in Fig. 4(a), is a triple band U-slotted patch using L-slot defected ground structure (DGS) [42]. Whereas Antenna II of Fig. 4(b) is a compact ultra-wideband (UWB) monopole antenna with radiator slots [43]. For both structures, the design goal is to minimize the maximum in-band reflection levels; the formulation of the design problems follows that of the second row of Fig. 1.

Antenna characteristics are evaluated using the transient solver of CST Microwave Studio. The model of Antenna II includes the SMA connector [44]. Table 2 presents the setup of variable-resolution EM models for both antennas: the lowest applicable resolution ($L_{min}$) and the highest one ($L_{max}$), along with the corresponding simulation times. The relationships between the model fidelity and the simulation time for both antennas are given in Fig. 5. The time evaluation ratios (fine/coarse model) equals 3.5

for Antenna I and 15 for Antenna II. This implies higher possible speedup to be obtained for the latter structure.

## 4.2 Setup and Numerical Results

Both verification structures have been optimized with the use of the PSO algorithm (swarm size $N = 10$, $k_{max} = 100$, the standard values of the control parameters, $\chi = 0.73$, $c_1 = c_2 = 2.05$, cf. [41]). Benchmarking included four versions of the proposed multi-fidelity algorithm (for the power factor $p = 1$, 2, 3, and 4), as well as single-fidelity basic PSO algorithm.

The results are provided in Table 3. Each algorithm has been run fifteen times independently. The algorithm performance is assessed using the following indicators: the average value of the merit function (i.e., the maximum in-band reflection), and its standard deviation, which serves to quantify solution repeatability. Algorithm cost-efficacy is assessed in terms of the overall execution time, as well as the savings w.r.t single-fidelity PSO algorithm. Figures 6 and 7 present the representative optimized antenna responses.
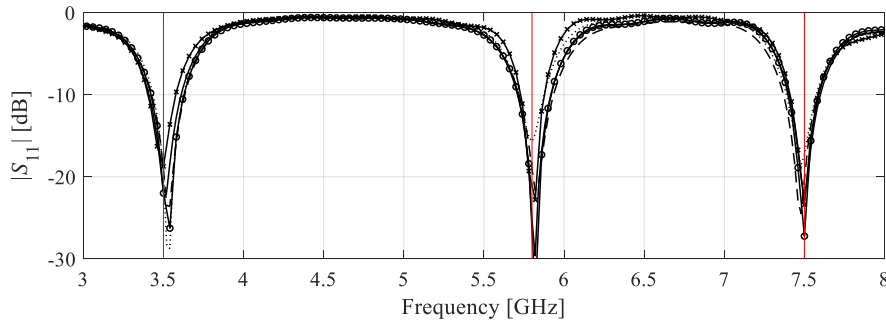


Fig. 6. Optimized designs of Antenna I for the representative runs of the single-fidelity procedure (——), as well as the proposed variable-fidelity algorithm: $p = 1$ (- - -), $p = 2$ (····), $p = 3$ (- o -), $p = 4$ (- x -). Target operating frequencies are indicated using vertical lines.
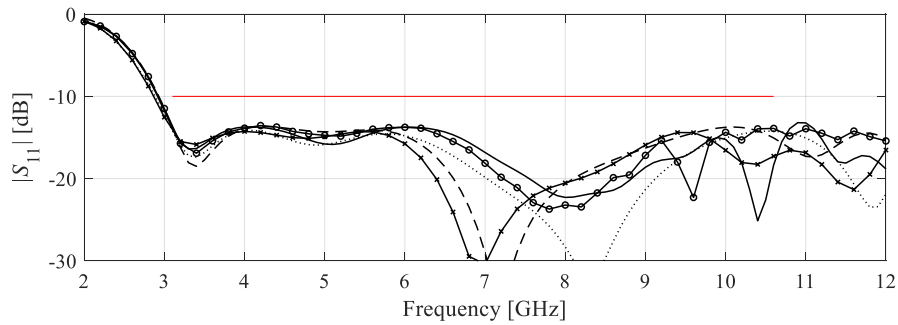


Fig. 7. Optimized designs of Antenna II for the representative runs of the single-fidelity procedure (——), as well as the proposed variable-fidelity algorithm: $p = 1$ (- - -), $p = 2$ (····), $p = 3$ (- o -), $p = 4$ (- x -). Target operating frequencies are indicated using vertical lines.

**Table 3.** Optimization results

| Algorithm setup | | Antenna I | | | | Antenna II | | | |
|---|---|---|---|---|---|---|---|---|---|
| | | Execution time [hours] | Savings[1] | $U$ [dB][2] | std($U$) [dB] | Execution time [hours] | Savings[1] | $U$ [dB][2] | std($U$) [dB] |
| High-fidelity ($L = L_{max}$) | | 31.7 | - | −15.7 | 2.5 | 105.1 | - | −13.1 | 1.6 |
| Variable resolution | $p = 1.0$ | 19.6 | 38.2 % | −18.4 | 2.1 | 45.6 | 56.6 % | −13.2 | 1.5 |
| | $p = 2.0$ | 16.5 | 47.9 % | −17.9 | 1.5 | 32.1 | 69.5 % | −13.0 | 1.6 |
| | $p = 3.0$ | 14.5 | 54.3 % | −15.8 | 2.2 | 26.3 | 75.0 % | −12.9 | 1.6 |
| | $p = 4.0$ | 13.4 | 57.7 % | −14.0 | 3.0 | 22.5 | 78.6 % | −12.5 | 1.7 |

[1]Percentage savings w.r.t. single-fidelity PSO algorithm
[2]Objective function value averaged over 15 algorithm runs

To verify the sample normality, we performed a Kolmogorov-Smirnov test for the merit function values rendered by consecutive algorithm runs: the null hypothesis that the results follow a normal distribution of the mean and standard deviation provided in Table 3 has not been rejected at the 5% significance level. Moreover, the typical $p$-values vary from 0.4 to 0.9. This corroborates that the (normalized) distribution of the merit function values is close to normal. This also indicates that the mean and standard deviation allow for reliable assessment of the algorithm performance.

### 4.3 Discussion

The following summary of the numerical results of Table 3 may be formulated:
- Considerable computational speedup w.r.t the single-fidelity procedure has been achieved through the employment of variable-resolution EM models into PSO optimization procedure. The actual level of cost-efficacy depends on the value of the power factor $p$. The lowest savings have been obtained for $p = 1$ (around 48 percent on average), whereas the highest ones have been reached for $p = 4$ (around 68 percent on average).
- The optimization process is reliable for the values of the power factor up 3. For higher $p$, the standard deviation of the merit function value increases, which implies deterioration of solution repeatability. Moreover, for both antennas, the $p > 3$ leads to degradation of the average merit function value.
- Observe that in this work, the computational budget for PSO algorithm is relatively low (1,000 objective function evaluations), even though the presented tasks are quite challenging. The reason for such a low budget is the necessity of maintaining practically acceptable CPU cost of the optimization procedure.

Overall, the employment of variable-resolution models leads to a considerable reduction in computational cost of the metaheuristic-based search without degrading design quality. Thus, the introduced algorithm may constitute an attractive alternative to direct metaheuristic-based optimization of antenna structures. The main advantages of our approach are simplicity of implementation and practically acceptable cost. At the

same time, it should be emphasized that the procedure is generic because the arrangement and handling of variable-resolution models is straightforward, here, realized using a single parameter of the EM solver selected for antenna evaluation.

## 5 Conclusion

This article investigated a possibility of reducing computational costs of nature-inspired antenna optimization by incorporating variable-resolution EM models. A simple model management scheme has been developed to adjust the fidelity of the antenna analysis. The search process starts with the lowest practically useful fidelity and gradually converges towards the high-fidelity representation upon the conclusion of the algorithm run. Different adjustment profiles have been tested. The proposed approach has been validated using several microstrip antennas. Extensive numerical experiments demonstrate up to eighty percent reduction of the computational costs with regard to the single-resolution algorithm without degrading the design quality.

## Acknowledgement

## References

1. Wang, Y., Zhang, J., Peng, F., Wu, S.: A glasses frame antenna for the applications in internet of things. IEEE Internet of Things J., **6**(5), pp. 8911–8918 (2019)

2. Le, T. T., Yun, T. -Y.: Miniaturization of a dual-band wearable antenna for WBAN applications. IEEE Ant. Wireless Propag. Lett., **19**(8), pp. 1452–1456 (2020)

3. Yuan, X. -T., Chen, Z., Gu, T., Yuan, T.: A wideband PIFA-pair-based MIMO antenna for 5G smartphones. IEEE Ant. Wireless Propag. Lett., **20**(3), pp. 371–375 (2021)

4. Xu, L., Xu, J., Chu, Z., Liu, S., Zhu, X.: Circularly polarized implantable antenna with improved impedance matching. IEEE Ant. Wireless Propag. Lett., **19**(5), pp. 876–880 (2020)

5. Ameen, M., Thummaluru, S. R., Chaudhary, R. K.: A compact multilayer triple-band circularly polarized antenna using anisotropic polarization converter. IEEE Ant. Wireless Propag. Lett., **20**(2), pp. 145–149 (2021)

6. Wong, K., Chang, H., Chen, J., Wang, K.: Three wideband monopolar patch antennas in a Y-shape structure for 5G multi-input–multi-output access points. IEEE Ant. Wireless Propag. Lett., **19**(3), pp. 393–397 (2020)

7. Shirazi, M., Li, T., Huang, J., Gong, X.: A reconfigurable dual-polarization slot-ring antenna element with wide bandwidth for array applications. IEEE Trans. Ant. Prop., **66**(11), pp. 5943–5954 (2018)

8.  Karmokar, D. K., Esselle, K. P., Bird, T. S.: Wideband microstrip leaky-wave antennas with two symmetrical side beams for simultaneous dual-beam scanning. IEEE Trans. Ant. Prop., **64**(4), pp. 1262–1269 (2016)

9.  Sambandam, P., Kanagasabai, M., Natarajan, R., Alsath, M. G. N., Palaniswamy, S.: Miniaturized button-like WBAN antenna for off-body communication. IEEE Trans. Ant. Prop., **68**(7), pp. 5228–5235 (2020)

10. Kovaleva, M., Bulger, D., Esselle, K. P.: Comparative study of optimization algorithms on the design of broadband antennas. IEEE J. Multiscale Multiphysics Comp. Techn., **5**, pp. 89–98 (20200

11. Genovesi., S., Mittra R., Monorchio, A., Manara, G.: Particle swarm optimization for the design of frequency selective surfaces. IEEE Ant. Wireless Propag. Lett., **5**, pp. 277-279 (2006)

12. Liang, S., Fang, Z., Sun, G., Liu, Y., Qu, G., Zhang, Y.: Sidelobe reductions of antenna arrays via an improved chicken swarm optimization approach/ IEEE Access, **8**, pp. 37664-37683 (2020)

13. Kim, S., Nam, S.: Compact ultrawideband antenna on folded ground plane. IEEE Trans. Ant. Prop., **68**(10), pp. 7179–7183 (2020)

14. Li, W., Zhang, Y., Shi, X.: Advanced fruit fly optimization algorithm and its application to irregular subarray phased array antenna synthesis. IEEE Access, **7**, pp. 165583–165596 (2019)

15. Jia, X., Lu, G.: A hybrid Taguchi binary particle swarm optimization for antenna designs. IEEE Ant. Wireless Propag. Lett., **18**(8), pp. 1581–1585 (2019)

16. Michalewicz, Z.: Genetic algorithms + data structures = evolution programs. Springer, New York (1996)

17. Wang, D., Tan, D., Liu, L.: Particle swarm optimization algorithm: an overview. Soft Computing, **22**, pp. 387–408 (2018)

18. Jiang, Z. J., Zhao, S., Chen, Y., Cui, T. J.: Beamforming optimization for time-modulated circular-aperture grid array with DE algorithm. IEEE Ant. Wireless Propag. Lett., **17**(12), pp. 2434–2438 (2018)

19. Baumgartner, P., Baurnfeind, T., Biro, O., Hackl, A., Magele, C., Renhart, W., Torchio, R.: Multi-objective optimization of Yagi-Uda antenna applying enhanced firefly algorithm with adaptive cost function. IEEE Trans. Magnetics, **54**(3), article no. 8000504 (2018)

20. Yang, S.H., Kiang, J.F.: Optimization of sparse linear arrays using harmony search algorithms. IEEE Trans. Ant. Prop., **63**(11), pp 4732–4738 (2015)

21. Li, X., Luk, K.M.: The grey wolf optimizer and its applications in electromagnetics. IEEE Trans. Ant. Prop., **68**(3), pp. 2186–2197 (2020)

22. Darvish, A., Ebrahimzadeh, A.: Improved fruit-fly optimization algorithm and its applications in antenna arrays synthesis. IEEE Trans. Antennas Propag., **66**(4), pp. 1756–1766 (2018)

23. Bora, T. C., Lebensztajn, L., Coelho, L. D. S.: Non-dominated sorting genetic algorithm based on reinforcement learning to optimization of broad-band reflector antennas satellite. IEEE Trans. Magn., **48**(2), pp. 767–770, 2012.

24. Cui, C., Jiao, Y., Zhang, L.: Synthesis of some low sidelobe linear arrays using hybrid differential eution algorithm integrated with convex programming. IEEE Ant. Wireless Propag. Lett., **16**, pp. 2444–2448 (2017)

25. Queipo, N.V., Haftka, R.T., Shyy, W., Goel, T., Vaidynathan, R., Tucker, P.K.: Surrogate-based analysis and optimization. Progress in Aerospace Sciences, **41**(1), pp. 1–28 (2005)

26. Easum, J.A., Nagar, J., Werner, P.L., Werner, D.H.: Efficient multi-objective antenna optimization with tolerance analysis through the use of surrogate models. IEEE Trans. Ant. Prop., **66**(12), pp. 6706–6715 (2018)

27. Liu, B., Aliakbarian, H., Ma, Z., Vandenbosch, G. A. E., Gielen , G., Excell, P.: An efficient method for antenna design optimization based on eutionary computation and machine learning techniques. IEEE Trans. Ant. Propag., **62**(1), pp. 7–18 (2014)

28. Alzahed, A.M., Mikki, S.M., Antar, Y.M.M.: Nonlinear mutual coupling compensation operator design using a novel electromagnetic machine learning paradigm. IEEE Ant. Wireless Prop. Lett., **18**(5), pp. 861–865 (2019)

29. Couckuyt, I., Declercq, F., Dhaene, T., Rogier, H., Knockaert, L.: Surrogate-based infill optimization applied to electromagnetic problems. Int. J. RF Microw. Computt.-Aided Eng., **20**(5), pp. 492–501 (2010)

30. Koziel, S., Pietrenko-Dabrowska, A.: Performance-based nested surrogate modeling of antenna input characteristics. IEEE Trans. Ant. Prop., **67**(5), pp. 2904–2912 (2019)

31. Koziel, S., Pietrenko-Dabrowska, A.: Performance-driven surrogate modeling of high-frequency structures. Springer, New York (2020)

32. Pietrenko-Dabrowska, A., Koziel, S.: Antenna modeling using variable-fidelity EM simulations and constrained co-kriging. IEEE Access, **8**(1), pp. 91048–91056 (2020)

33. Koziel, S., Pietrenko-Dabrowska, A.: Expedited feature-based quasi-global optimization of multi-band antennas with Jacobian variability tracking. IEEE Access, **8**, pp. 83907–83915 (2020)

34. Koziel, S.: Fast simulation-driven antenna design using response-feature surrogates. Int. J. RF & Micr. CAE, **25**(5), pp. 394–402 (2015)

35. Koziel, S., Bandler, J.W.: Reliable microwave modeling by means of variable-fidelity response features. IEEE Trans. Microwave Theory Tech., **63**(12), pp. 4247–4254 (2015)

36. Rayas-Sanchez, J. E.: Power in simplicity with ASM: tracing the aggressive space mapping algorithm over two decades of development and engineering applications. IEEE Microwave Mag., **17**(4), pp. 64–76 (2016)

37. Koziel, S., Unnsteinsson, S.D.: Expedited design closure of antennas by means of trust-region-based adaptive response scaling. IEEE Antennas Wireless Prop. Lett., **17**(6), pp. 1099–1103 (2018)

38. Li, H., Huang, Z., Liu, X., Zeng, C., Zou, P.: Multi-fidelity meta-optimization for nature inspired optimization algorithms. Applied Soft. Comp., **96**, Art. 106619 (2020)

39. Tomasson, J.A., Pietrenko-Dabrowska, A., Koziel, S.: Expedited globalized antenna optimization by principal components and variable-fidelity EM simulations: application to microstrip antenna design. Electronics, **9**(4), Art. 673 (2020)

40. Koziel, S., Ogurtsov, S.: Model management for cost-efficient surrogate-based optimization of antennas using variable-fidelity electromagnetic simulations. IET Microwaves Ant. Prop., **6**(15), pp. 1643–1650 (2012)

41. Kennedy, J., Eberhart, R.C.: Swarm Intelligence, Morgan Kaufmann, San Francisco (2001)

42. Consul, P.: Triple band gap coupled microstrip U-slotted patch antenna using L-slot DGS for wireless applications. Communication, Control and Intelligent Systems (CCIS), Mathura, India, pp. 31-34 (2015)

43. Haq, M.A., Koziel, S.: Simulation-based optimization for rigorous assessment of ground plane modifications in compact UWB antenna design. Int. J. RF Microwave CAE, **28**(4), e21204 (2018)

44. SMA PCB connector, 32K101-400L5, Rosenberger Hochfrequenztechnik GmbH & C. KG (2021)